DEUTSCHES ELEKTRONEN-SYNCHROTRON DESY

DESY 85-063
July 1985

A STUDY OF 3-JET EVENTS IN e^+e^- ANNIHILATION INTO HADRONS AT 34.6 C.M. ENERGY

by

TASSO Collaboration

ISSN 0418-9833

NOTKESTRASSE 85 · 2 HAMBURG 52

To be sure that your preprints are promptly included in the
HIGH ENERGY PHYSICS INDEX ,
send them to the following address (if possible by air mail) :

DESY
Bibliothek
Notkestrasse 85
2 Hamburg 52
Germany

DESY 85-063
July 1985

ISSN 0418-9833

A STUDY OF 3-JET EVENTS IN e^+e^- ANNIHILATION INTO HADRONS AT 34.6 C.M. ENERGY

TASSO Collaboration

M.Althoff, W.Braunschweig, F.J.Kirschfink, H.U. Martyn, R.Rosskamp, D.Schmitz, H.Siebke[1], W.Wallraff
I.Physikalisches Institut der RWTH Aachen, 5100 Aachen, Germany[14]

J.Eisenmann, H.M.Fischer, H.Hartmann, A.Jocksch, G.Knop, H.Kolanoski, H.Kück[2], V.Mertens, R.Wedemeyer
Physikalisches Institut der Universität Bonn, 5300 Bonn, Germany[14]

B.Foster, A.Wood
H.H.Wills Physics Laboratory, University of Bristol, Bristol BS8 1TL, UK[15]

E.Bernardi, Y.Eisenberg[3], A.Eskreys[4], R.Fohrmann, K.Gather, H.Hultschig, P.Joos, U.Karshon[3], B.Klima, U.Kötz, H.Kowalski, A.Ladage, B.Löhr, D.Lüke, P.Mättig[5], G.Mikenberg[3], D.Notz, J.Pyrlik[6], W.Schütte, D.Trines, T.Tymieniecka[7], G.Wolf[8], W.Zeuner
Deutsches Elektronen-Synchrotron, DESY, 2000 Hamburg, Germany

E.Hilger, T.Kracht, H.L.Krasemann, E.Lohrmann, D.Pandoulas[9], G.Poelz, K.U.Pösnecker
II. Institut für Experimentalphysik der Universität Hamburg, 2000 Hamburg, Germany[14]

D.M.Binnie, P.J.Dornan, D.A.Garbutt, C.Jenkins, W.G.Jones, J.K.Sedgbeer, D.Su, J.Thomas, W.A.T.Wan Abdullah[10],
Department of Physics, Imperial College, London SW7 2AZ, UK[15]

F.Barreiro[11], L.Labarga, E.Ros
Universidad Autonoma de Madrid, Madrid, Spain[18]

M.G.Bowler, P.Bull, R.J.Cashmore, P.Dauncey, R.Devenish, C.M.Hawkes, G.Heath, D.J.Mellor,
Department of Nuclear Physics, Oxford University, Oxford OX1 3RH, UK[15]

S.L.Lloyd
Department of Physics, Queen Mary College, London E1 4NS, UK[15]

K.W.Bell, G.E.Forden, J.C.Hart, D.K.Hasell, D.H.Saxon
Rutherford Appleton Laboratory, Chilton, Didcot, Oxon OX11 0QX, UK[15]

S.Brandt, M.Dittmar, M.Holder, G.Kreutz, B.Neumann
Fachbereich Physik der Universität-Gesamthochschule Siegen, 5900 Siegen, Germany[14]

E.Duchovni, A.Montag, R.Mir, D.Revel, E.Ronat, G.Yekutieli. A.Shapira
Weizmann Institute, Rehovot 76100 , Israel[16]

G.Baranko[12], A.Caldwell, M.Cherney, M.Hildebrandt, J.M.Izen, M.Mermikides, S.Ritz, G.Rudolph[12], D.Strom, M.Takashiba, H.Venkataramania[13], E.Wicklund, Sau Lan Wu, G.Zobernig
Department of Physics, University of Wisconsin, Madison, WI 53706, USA[17]

[1] Now at DEC, Hamburg, Germany
[2] Now at Fraunhofer Institut, Duisburg, Germany
[3] On leave from Weizmann Institute, Rehovot, Israel
[4] On leave from Institute of Nuclear Physics, Cracow, Poland
[5] Now at IPP Canada, Carleton Univeristy, Ottawa, Canada
[6] Now at University of Texas, Austin, USA
[7] On leave from Warsaw University, Poland
[8] Now at SLAC, Stanford, CA, USA
[9] Now at I.Physikalisches Institut der RWTH Aachen, 5100 Aachen, Germany
[10] On leave from University of Malaya, Kuala Lumpur
[11] Now at University of Siegen, Germany
[12] Now at Institut für Experimentalphysik der Universität Innsbruck, Austria
[13] Now at Yale University, New Haven, CT, USA

[14] Supported by the Bundesministerium für Forschung und Technologie
[15] Supported by the UK Science and Engineering Research Council
[16] Supported by the Minerva Gesellschaft für Forschung mbH
[17] Supported by the US Department of Energy, contract DE-AC02-76ER00881
[18] Supported by CAICYT

Abstract

Three-jet events produced by e^+e^- annihilation into hadrons at 34.6 GeV c.m. energy were studied by comparing them with 2nd order QCD and two different models of fragmentation. The distribution of low energy particles in the 3-jet plane is found to be better described by the LUND color string model than by the independent jet model. The opposite is true for more energetic particles flowing between the 3 jets. The average transverse momenta in jets can be described with values of σ_q between 350 and 500 MeV/c for the gluon jet.

Introduction

The two-jet dominance of the one-photon annihilation process $e^+e^- \to$ hadrons can be understood as quark pair production $e^+e^- \to q\bar{q}$ and subsequent jet formation. At c.m. energies above ~30 GeV, clearly resolved 3-jet events have been detected [1] with a rate of about 10%. They were successfully explained [2] in the framework of perturbative QCD as arising from hard non-collinear gluon bremsstrahlung, $e^+e^- \to q\bar{q}g$, and subsequent fragmentation into hadrons. The lowest energy jet is expected to be the gluon jet with ~50% probability. Thus, the 3-jet events constitute a suitable laboratory to test different schemes of quark and gluon fragmentation.

The Independent Jet (IJ) model [3] assumes that quarks and gluons fragment independently of each other and that the axes of fragmentation are the original parton directions. In contrast, the color string model developed by the LUND group [4] assumes that the fragmentation occurs along the color flux lines which connect the quark and the antiquark via the gluon. The angular distribution of hadronic energy in the $q\bar{q}g$ plane differs in the two models. The distinctive prediction of the LUND model is that the angular region between the q and $\bar{q}$ directions is relatively depleted of particles. Experimental analyses by the JADE collaboration [5] and, more recently, by the PEP-4 TPC collaboration [6] showed that the LUND model is superior to the IJ model in describing the angular energy flow. The IJ model cannot be tuned to simulate the "string effect". It is interesting to note that the QCD shower model due to Webber [7] which includes soft gluon interference effects, is also able to reproduce this feature of the data [6, 8].

The important question of whether quarks and gluons fragment differently has been investigated at high energy e^+e^- and $p\bar{p}$ colliders. From $e^+e^- \to$ 3 jets, the JADE collaboration [9] concluded that gluon jets have wider transverse momentum and softer longitudinal momentum distributions than quark jets, as predicted by the LUND model. Jets produced with high transverse energy E_T at the CERN $p\bar{p}$ collider are expected to consist mostly of gluon jets at the lower end of the measured jet energy range. A first comparison [10] of quark jets from PETRA with high - E_T

jets from the UA1 experiment revealed no striking differences in the distribution of the scaled longitudinal momentum. The UA2 collaboration presented evidence [11] that gluon jets have higher charged multiplicity than quark jets. Their E_T flow distribution is consistent with a QCD shower model in which gluon jets are intrinsically broader than quark jets.

In the present paper, we investigate a selected sample of events of the type $e^+e^- \to$ 3 jets collected with the TASSO detector at c.m. energies around 35 GeV. In section 2, our method of selecting 3-jet events is described. In section 3, we discuss the Monte Carlo models with which the data are compared. The angular distribution of particles in the plane spanned by the 3 jets is studied in section 4 with the aim of differentiating between the IJ and the LUND models. The influence which 4-jet events can have on our results is also discussed. In section 5 we deal with the question of whether quark and gluon jets differ in average transverse momentum. Our conclusions are given in section 6.

2. Selection of 3-jet events

The data were taken with the TASSO detector at the e^+e^- storage ring PETRA at center-of-mass energies W between 33 and 36.6 GeV, the average being $\bar{W}$ = 34.6 GeV. The selection of multihadronic annihilation events is identical to that described in [12]. From the information on charged particles a total of 21 484 events are accepted. In addition, three further cuts are made: (a) events are removed for which the sum of the particle momenta $\Sigma|p|$ exceeds 2W; (b) the angle θ_s between the sphericity axis and the beam direction is required to satisfy $|\cos\theta_s| < 0.85$; (c) the angle θ_N between the normal to the event plane and the beam direction has to satisfy $|\cos\theta_N| > 0.1$ in order to reject badly reconstructed events and events with a hard photon radiated from the e^+ or e^-. The number of events remaining after these cuts is 18 846.

The event plane $(\hat{n}_2, \hat{n}_3)$ is found by diagonalizing the momentum tensor [13] yielding eigenvalues $Q_1 < Q_2 < Q_3$ and corresponding eigenvectors $\hat{n}_1, \hat{n}_2, \hat{n}_3$. Only the charged tracks are used in the analysis. The method

of generalized sphericity [14] is used to resolve each event into 3 non-overlapping sets of particles and to determine the jet axes. This method uses only the components of momentum projected into the event plane and requires the sum of the reduced sphericities

$$\sum_{j=1}^{3} S_j' = \sum_{j=1}^{3} \sum_k (p_{T\,in}^2)_k \Big/ \sum_k (p_{in}^2)_k \qquad (1)$$

to be a minimum where k runs over the particles of jet j. Here, p_{in} is the particle momentum projected into the event plane and $p_{T\,in}$ is the component of p_{in} transverse to the jet axis $\hat{k}_j$ of the jet to which the particle is assigned:

$$p_{in} = \sqrt{p^2 - p_{T\,out}^2}\,, \quad p_{T\,in} = \sqrt{p_{in}^2 - p_{||}^2}\,.$$

Here, p is the modulus of the particle momentum, $p_{T\,out}$ is the component perpendicular to the event plane and $p_{||}$ is the component parallel to the jet axis $\hat{k}_j$:

$$p_{T\,out} = |\vec{p} \cdot \hat{n}_1|, \quad p_{||} = |\vec{p} \cdot \hat{k}_j|.$$

The jet axis $\hat{k}_j$ associated with each jet j is defined as the direction in the event plane for which the quantity $\Sigma p_{T\,in}^2 / \Sigma p_{in}^2$ is a minimum. The relative angles between the jet axes are denoted by $\Phi_{ij} = \Phi_i - \Phi_j$ where Φ_i is the azimuthal angle of jet i in the event plane. The definition of variables is illustrated in Fig. 1a.

Given the 3 sets of particles, we select 3-jet event candidates by energy-angle cuts:

(i) Each jet has to have a visible scaled energy $x_{vis} > 0.12$, where $x_{vis} = E_{vis}/E_{beam}$ and E_{vis} is the sum of the particle energies assuming the particles to be pions. This cut corresponds roughly to $E_{vis} > 2$ GeV, reducing the data sample to 11 787 events. No cut on the jet multiplicity was made. The fraction

of jets consisting of only one track is 2.6% in the final sample.

(ii) To ensure good separation of the jets we require $|\Phi_{ij}| > 55^{\circ}$. This cut leaves 3507 events.

(iii) If a line in the event plane exists such that all 3 jets are on one side of this line, then the event represents momentum imbalance and is rejected. 3240 events survive this cut.

(iv) Under the assumption of massless jets and neglecting radiation in the initial state, the angles Φ_{ij} are used to reconstruct the scaled jet energies

$$x_{i\ rec} = 2 \sin \Phi_{jk} / (\sin \Phi_{12} + \sin \Phi_{23} + \sin \Phi_{31}) \qquad (2)$$
$$= E_{i\ rec} / E_{beam} \qquad i,j,k = 1,2,3 \text{ and cyclic}$$

Each jet is then required to satisfy $x_{i\ rec} > 0.24$, corresponding to more than 4 GeV of energy.

The 3-jet selection cuts (i)-(iv) are satisfied by $N_{3jet} = 2361$ events, or 12.5% of 18 846 hadronic events. It is seen that cut (ii) has the strongest effect. The results presented in this paper do not depend on the precise values of the cuts (i), (ii) and (iv). Since the number of jets is fixed to 3 by the method of generalized sphericity, events with 4 or more jets in the final state may also pass the selection cuts (i)-(iv). This will be discussed in sect. 4a.

3. Model Calculations

In order to interpret the experimental distributions, they are compared with Monte Carlo model calculations. The Monte Carlo models include radiative effects in the initial state [15], perturbative QCD to 2nd order in α_s [16, 17], fragmentation, decay of unstable particles and a detailed detector simulation. The model events are subjected to the same cuts as the real data. Several large samples of Monte Carlo events (60 000 accepted

hadronic events each) were generated using the LUND string model [18] and several variants of the IJ model to describe fragmentation. The most important parameters+) of these models have already been determined [19] by fitting to all hadronic events. Table 1 summarizes the variants of the IJ model together with the parameter values used. In model 2, the gluon is assumed to fragment like a light quark (IJ g=q). The transverse (longitudinal) momentum distribution in a gluon jet is varied through the parameter $\sigma_{q,g}$ (a_g), see models 1, 3, 4 (model 5). We also consider gluon splitting $g \to q\bar{q}$ à la Altarelli-Parisi (model 6), and changing the fragmentation functions of both quark and gluon jets (model 7). The possible influence on our results of the specific procedure to enforce overall energy-momentum balance (we use the Lorentz boost method as described in [22]) is studied by generating an event sample in which energy-momentum is conserved only on average (not event-by-event).

The parton configuration is generated according to 2nd order QCD including virtual corrections (Extended FKSS [17, 19]). The cut-off procedure applied to 3- and 4- parton events is of the Sterman-Weinberg type with parameters $\varepsilon = 0.20$ and $\delta = 40^{\circ}$, i.e. the energy of each parton has to exceed $0.20\ E_{beam}$ and the angle between any pair of partons has to exceed 40°. Note that our experimental cuts (ii) and (iv) are of the same type. For the strong coupling constant we have chosen $\alpha_s = 0.155$ (0.205) in case of IJ (LUND) fragmentation, which are median values over various methods of determination [19]. After applying cuts (i)-(iv) to the Monte Carlo events, the percentages of $q\bar{q}$, $q\bar{q}g$ and $q\bar{q}gg + q\bar{q}q\bar{q}$ events are 6%, 71% and 23% (3%, 69% and 28%) for the IJ (LUND) models respectively. The fraction of

---

+) The fitted value of a_q occurring in the primordial fragmentation function $(1 - z)^{a_q}$ of light quarks is 0.61 (0.42) for the IJ (LUND) model, where z is defined in [19]. For heavy quarks (c and b) the parametrization of [20] is taken. The fitted value of the transverse momentum parameter $\sigma_{q,q}$ for quark jets is 0.35 (0.32) GeV/c for the IJ g=q (LUND) model. The production ratio of $J^P = 0^-$ mesons to the sum of $J^P = 0^-$ and 1^- mesons is set to 0.42 in both models [21].

hadronic events passing these cuts is 13.3% (13.5%) for the IJ (LUND) models, to be compared with 12.5% for the data.

The distributions of the variables x_{vis}, min Φ_{ij} and x_{rec} on which the cuts (i), (ii) and (iv) have been applied, are displayed in Figs. 2a, b, c for the selected 3-jet event sample. QCD is seen to provide a good description of the jet angle and energy distributions, independent of the fragmentation scheme used. The contribution from gluon jets is drawn as dotted line in Fig. 2c showing gluon enrichment at the lower jet energies.

The Monte Carlo simulation can be used to estimate the experimental resolution of the jet angle determination. For this purpose we select events generated as $q\bar{q}g$ without an initial state photon. The reconstructed jets are compared with the original parton directions. The r.m.s. resolution of the jet angle Φ (or the jet energy x_{rec}) is 15° (0.12) near $x_{rec} = 0.30$ and decreases to 6° (0.06) near $x_{rec} = 0.95$. The main sources of these errors are the fluctuation of the charged particle component of the jets, detector effects and uncertainties of the jet analysis.

4. Test of Independent Jet versus String Fragmentation

As originally suggested in [23], the particle distribution in the event plane in 3-jet events constitutes a sensitive area to discriminate experimentally between the IJ and the LUND models. The IJ model assumes that the partons q, $\bar{q}$ and g of a 3-jet event fragment independently of each other in the center-of-mass system of $q\bar{q}g$. The parton directions are taken as the axes of fragmentation. In contrast to this, the LUND model assumes that the fragmentation takes place in the rest systems of two independent color strings which are stretched between q-g and between g-$\bar{q}$. A similar prescription exists for $q\bar{q}gg$ events. The produced hadrons are Lorentz-boosted with respect to the $q\bar{q}g$ rest system because of the motion of the strings. Consequently, the particle density in the middle of the q-$\bar{q}$ angular region relative to the densities in the q-g and g-$\bar{q}$ regions is considerably smaller (by a factor ~2.5 or more, depending on the kinematics) than in the IJ model. This asymmetry, which will be studied in sect. 4a, is

however diminished in practice because the gluon jet can be positively identified through energy ordering in only ~50% of the cases.

In sect. 4b, we present another way to test the predictions of the LUND model. Correlations between angle and momentum of particles within a jet are studied. In the LUND model, the soft particles preferentially point towards the gluon direction while the hard particles approximately keep the original parton directions. In IJ models, all particles point on average into the direction of the partons from which they were emitted. Deviations from this alignment may arise from effects of overall energy-momentum balance.

4a. Azimuthal Particle Flow

In this section we study the distribution of the azimuthal angle ψ of charged particles projected into the event plane. The measured jets are ordered according to their energy, $x_{1\,rec} > x_{2\,rec} > x_{3\,rec}$, and the event is oriented as shown in Fig. 1a. The most energetic jet (#1) defines $\psi=0$. According to QCD, the least energetic jet (#3) has the highest chance to be a gluon jet: the jets 1, 2 and 3 are gluon jets in 15%, 31% and 57% of the cases, respectively, almost independent of the fragmentation model. Note that due to the presence of $q\bar{q}gg$ events, these percentages sum up to more than 100%.

It is convenient to eliminate the effect of the event-to-event variation of the angles Φ_{ki} between jets by introducing the reduced azimuthal angle [5]

$$\psi_j' = \frac{\psi - \Phi_i}{\Phi_k - \Phi_i} \qquad i,j,k = 1,2,3 \text{ and cyclic} \qquad (3)$$

where the particle under consideration is located between jets i and k ($\Phi_i < \psi < \Phi_k$). The angles ψ_j' therefore run from 0 to 1. The index j denotes the angular region opposite to jet j, see Fig. 1a.

The experimental distributions of ψ_2', ψ_1' and ψ_3' are shown in Fig. 3a, for all particle momenta. The density is highest near the jet directions ($\psi' = 0$ or 1). The model calculations superimposed on the data are normalised to the same number of 3-jet events ($= N_{3jet}$). The jet peaks are seen to be well described by both the IJ q=q and the LUND models. Differences between data and models and among the models occur mainly in the valley between jets 1 and 2 which are expected to be q or $\bar{q}$ jets most of the time. The particle density in that valley is seen to be lower than expected from independent fragmentation. The data prefer the LUND model. The same observation was made in the ψ distribution itself (not shown).

Possible systematic errors are expected to be less important if, instead of absolute particle densities, ratios of particle densities are considered. Denote by N(j) the number of particles flowing into the gap region defined by $0.25 < \psi_j' < 0.75$ opposite to jet j. We take the densities N(1) and N(2) on either side of jet 3 and divide them by the density N(3) opposite to jet 3. The ratios N(2)/N(3) and N(1)/N(3) are given in Table 2 for the data and for various models. It is seen that none of the variants of the IJ model listed in this table is able to reproduce the data. Changing the transverse or longitudinal fragmentation functions of the gluon jet within the IJ scheme has very little effect on these ratios, while the absolute densities do depend on the gluon fragmentation function. The scheme used by us to conserve total energy-momentum has negligible effect on the ratios. On the other hand, the results of the LUND model are in better agreement with the data, although somewhat too high, and are clearly distinct from those computed with IJ models. The errors given in Table 2 are statistical only. From studies with different detector simulations we assign a systematic error of 0.06 to the Monte Carlo model numbers.

Next we investigate the momentum dependence of the density ratios. Figs. 4a and b show N(2)/N(3) and N(1)/N(3) in intervals of $x_{in} = p_{in}/E_{beam}$ where p_{in} is the particle momentum projected into the event plane. We limit the analysis to $x_{in} < 0.1$ for reasons of statistics. The density ratios are seen to depend sensitively on the momentum. The N(2)/N(3) data rise in the soft particle region, $x_{in} < 0.04$, and stay constant or decrease beyond 0.04. The ratio N(1)/N(3) rises strongly with x_{in}. The data in the soft particle region, $x_{in} < 0.04$, are well described by the LUND string model whereas the

IJ model can be ruled out in this region. In contrast, the data for x_{in} values above 0.04 are not as high as predicted by the LUND model but rather follow the IJ model.

This deviation of the LUND model from the data is now studied in more detail since it has not been reported previously. We note that our cuts to select a sample of 3-jet events differ from those used by the JADE [5] and PEP-4 TPC [6] groups, who applied cuts in the Q-plot (planarity $P = Q_2 - Q_1 > P_{cut}$ and aplanarity $Q_1 < Q_{1\,cut}$). We found that only the planarity cut has significant influence on the results. Figs. 4c and 4d show N(2)/N(3) versus x_{in} for our 3-jet event sample requiring in addition $P < 0.07$ or $P > 0.07$. This value of P_{cut} was used by JADE [5]. The values of N(2)/N(3) are seen to be very different for the two regions of planarity. It is also seen that the sensitivity to string-like effects is enhanced in low planarity events. These events are characterized by a lower average energy of jet 3 and consequently a higher probability that jet 3 is the gluon jet. It is remarkable that the data-LUND discrepancy in the momentum region $0.04 < x_{in} < 0.10$ is much more pronounced in the low planarity sample. This provides the likely explanation for why both JADE and PEP-4 TPC observed perfect agreement of their data with the LUND model. A similar result is obtained if instead of a cut in the planarity, a cut in the energy x_j of the least energetic jet is applied. We verified that this discrepancy between data and LUND model is not caused by experimental problems like badly reconstructed tracks and is not affected by changes of the detector simulation. We also varied the definition of the angular gaps within the range $0.2 < \psi_j' < 0.8$ and $0.3 < \psi_j' < 0.7$ and found the conclusions to be unchanged.

In order to see in which of the angular regions the deviations of the models from the data occur, we show in Figs. 3b and 3c the ψ_j' distributions separately for $x_{in} < 0.04$ and for $0.04 < x_{in} < 0.10$. The IJ model obviously produces too many soft particles in the valley between jets 1 and 2 (Fig. 3b) but is in better agreement with the data at higher momenta (Fig 3c). The LUND model prediction for the valley between jets 1 and 2 is slightly below the data in both momentum regions.

In the following we investigate the possible influence on our results from 4-jet events. The idea is that particles emitted between the three jet axes, especially the more energetic ones, could belong to a fourth jet. We use a cluster algorithm [24] which is able to determine the number of jets in an event. Clusters of visible energy $E_{vis} > 0.12\ E_{beam}$ separated from any other clusters by more than 45^{o} are called jets. The fraction of 4-jet events within our "3-jet" event sample found in the data, the LUND model and the IJ model is 10%, 7% and 7%, respectively. Of the 7% Monte Carlo events, only about one half originate from genuine 4-parton events. The corresponding numbers for 5-jet events are 1%, 0.3% and 0.5%. Fig. 4e shows the particle density ratio N(2)/N(3) without the contribution from 4- and 5-jet events. Compared with Fig. 4a, the main features are the same except that the statistical errors are larger for the data points at higher momenta. The density ratios averaged over all momenta show that the LUND model is in better agreement with the data if events with 4 or more jets are removed (Table 2).

In this context we remark that the model predictions for the density ratios depend on the order of the perturbative QCD calculation. For example, N(2)/N(3) as calculated from the LUND model has the value 1.39 for $q\bar{q}g$ events and only 1.11 for $q\bar{q}gg + q\bar{q}q\bar{q}$ events. This is true for events passing the 3-jet selection cuts (i)-(iv). It is conceivable that the inclusion of even higher order QCD terms would further reduce the density ratios.

We also looked for a possible dependence of the particle flow ratios N(2)/N(3) and N(1)/N(3) on the momentum component $|p_{T\ out}|$ perpendicular to the event plane. In the LUND model, one expects these ratios to increase with increasing $|p_{T\ out}|$. Neither the data nor the model calculations show any variation. Monte Carlo studies using the LUND model have shown that in our data the effect which actually exists at the generator level, disappears through the combined effects of radiative corrections and of 3-jet analysis.

4b. Jet Directions

The analysis discussed in this section is sensitive to the correlation, within a given jet, between the direction and the momentum of the particles. No identification of the gluon jet is required. So far, the jet directions were computed by the method of generalized sphericity. For the purpose of this study, we redefine the jet axes by momentum weighted vector sums [23]

$$\hat{k}_j^{(n)} \propto \sum |p_{in}|^{n-1}\, \vec{p}_{in}\ , \qquad j = 1,2,3 \qquad (4)$$

where the sum runs over the tracks associated with jet j. The assignment of particles to jets is taken from the result of the generalized sphericity algorithm and is not changed. For small values of n and n > 0, the soft particles are important relative to the hard particles and are of decreasing importance as n increases.

In order to measure the change of the 3-jet kinematics upon changing the power n, we construct the variable $\Delta x_T^{(n)}$ which is defined once per event. From the relative angles between the $\hat{k}_j$ of eqn. (4), the fractional jet energies $x_{j\ rec}^{(n)}$ are computed as in eqn. (2). The jets are renumbered such that $x_{1\ rec}^{(n)} > x_{2\ rec}^{(n)} > x_{3\ rec}^{(n)}$. Out of the two independent kinematic variables characterizing a 3-body state, we choose $x_T^{(n)}$ which is defined as the transverse momentum of jet 3 with respect to jet 1, divided by the beam energy, see Fig. 1b for illustration. We define the change of x_T as

$$\Delta x_T^{(n)} = x_T^{(2)} - x_T^{(n)} \qquad (5)$$

where n = 2 is chosen as a reference point.

Fig. 5a shows $\Delta x_T^{(n)}$ averaged over the events of the 3-jet sample for values of n in the range $\frac{1}{2} \leq n \leq 4$. The numbers for n = 1 and n = 3 are also given in Table 3. Strong statistical correlations exist among the data points since the same information is used for each n. The effects seen in Fig. 5a are small: the size of $\langle \Delta x_T^{(n)} \rangle$ is ~1/10 of the standard deviation of $\Delta x_T^{(n)}$ and is only ~1/100 of the average value of $x_T^{(n)}$ which is about 0.33. From changes of the detector simulation, we estimate the systematic error of the model results to be equal to or smaller than the Monte Carlo

statistical error. The comparison of the data to model predictions in Fig. 5a shows a pattern similar to that of the azimuthal flow analysis of the previous section. For low n-values ($n < 2$) the LUND model describes the data quite well while the IJ model fails grossly. This deficiency of the IJ model cannot be cured by giving the gluon jet a softer or broader fragmentation spectrum as is evident from Table 3. The IJ model deviates even more from the data if exact energy-momentum balance is not imposed. At high n-values ($n > 2$) the prediction of the LUND model gradually deviates from the data. The data are lying in between the two model curves. Fig. 5b and Table 3 show that the agreement of the high n data with the LUND model gets better if events with more than 3 jets in the final state are removed. The same cluster algorithm as that described in sect. 4a was used.

As an example, Fig. 6 shows the distribution of $\Delta x_T^{(1)}$. The peak position and the width are well described by the LUND model. The IJ model histogram is displaced with respect to the data.

The effect of the LUND color string on the variable $\Delta x_T^{(n)}$ can be qualitatively understood as follows. Consider e.g. the calculation of $\Delta x_T^{(1)} = x_T^{(2)} - x_T^{(1)}$. In LUND $q\bar{q}g$ events, low momentum particles are preferentially emitted into the q-g and $\bar{q}$-g angular sectors as compared to the q-$\bar{q}$ sector. Going from $n = 2$ to $n = 1$, i.e. increasing the weight given to low momentum particles, the angle between the reconstructed q and $\bar{q}$ jets moves closer to 180°. In other words, the kinematic configuration becomes more 2-jet like. This implies $x_T^{(1)} < x_T^{(2)}$ or $\Delta x_T^{(1)} > 0$, on average. In $q\bar{q}g$ events with IJ fragmentation one would naively expect $\langle \Delta x_T^{(1)} \rangle = 0$, because low and high momentum particles emitted from a parton go into the same direction, on average. The jet finding method, however, disturbs the rotational symmetry around the jet axis such that $x_T^{(1)} > x_T^{(2)}$. Of course, this distortion also acts on LUND events. The net effect of the color string is thus $\langle \Delta x_T^{(n)} \rangle_{LUND} > \langle \Delta x_T^{(n)} \rangle_{IJ}$ for $n < 2$ and vice versa for $n > 2$, as observed in Fig. 5a.

We checked the possible influence on the results from momentum smearing which becomes increasingly important at high momenta and therefore at high n. Removing the small portion (9%) of events having at least one track with $|p| > E_{beam}/2$ does not significantly alter the data and Monte Carlo results displayed in Fig. 5a.

Further searches for possible systematic errors arising from imperfections of the detector simulation were performed by splitting the 3-jet event sample into two equally large samples according to the following criteria: different orientations of the events in the detector volume were selected by $|\cos \theta_s| \lesssim 0.45$ and $|\cos \theta_N| \lesssim 0.65$; different ranges of visible event energy were selected by $\Sigma|p|/W \lesssim 0.53$. For each of these sub-samples, the jet direction and the azimuthal angle analyses were performed. It was found that the "string -effect" is present in each of the data sub-samples. This is also true for the deviations of the LUND model from the data discussed above. We find no evidence for serious systematic errors.

An analysis similar to our $\Delta x_T^{(n)}$ analysis was performed by the JADE collaboration [5]. They plotted $\langle p_{T\ in} \rangle$ against $p_{||}$ for each jet, where $p_{T\ in}$ can be positive or negative. Repeating this kind of analysis, we arrive at the same conclusions as those given above.

5. Transverse Momenta in Jets

In this section we investigate the important question of whether quark and gluon jets differ in their average transverse momenta $\langle p_T \rangle$. This is done by comparing the data with IJ model calculations. Only in this model, $\langle p_T \rangle_{gluon}$ can be adjusted independently of $\langle p_T \rangle_{quark}$ by means of the parameters $\sigma_{q,g}$ and $\sigma_{q,q}$. The transverse momenta $p_{T\ out}$ and $p_{T\ in}$ of charged particles in jets were defined in eqn. (1). We use the square of p_T because it turned out to be more sensitive than p_T to variations of the model parameters $\sigma_{q,g}$ and $\sigma_{q,q}$. Since we are interested in possible differences between quark and gluon jets, we consider the following ratios

$$r_{out} = \langle p_{T\ out}^2 \rangle_g \ / \ \langle p_{T\ out}^2 \rangle_q$$
$$r_{in} = \langle p_{T\ in}^2 \rangle_g \ / \ \langle p_{T\ in}^2 \rangle_q \qquad (6)$$

were the subscripts "g" and "q" denote gluon enriched and quark enriched energy regions which we define as $0.3 < x_{rec} < 0.6$ and $0.8 < x_{rec} < 0.96$, respectively. The estimated gluon content is 55% and 15%, respectively, see also Fig. 2c. The advantage of using the ratios (6) instead of the average transverse momenta themselves is that they are insensitive to uncertainties in the fine tuning of the quark jet parameter $\sigma_{q,q}$ as long as $\sigma_{q,q} \propto \sigma_{q,g}$. We fix $\sigma_{q,q}$ to 0.35 GeV/c which is the value derived from the total hadronic event sample. The ratios are then expected to change if the gluon jet parameter $\sigma_{q,g}$ is changed. This is seen in Fig. 7 where r_{out} and r_{in} are plotted for the data and for several values of $\sigma_{q,g}$. Saturation is seen to occur in case of r_{in} above $\sigma_{q,g} \approx 0.50$ GeV/c due to increasing overlap of jets in the event plane. Within 2 standard deviations, the IJ model provides an acceptable description of both the r_{out} and r_{in} data in the parameter range $0.35 \lesssim \sigma_{q,g} \lesssim 0.50$ GeV/c. This means, our data are consistent with the hypothesis that the gluon jet has the same or larger average transverse momentum (within the range given) than the quark jet. The values of Fig. 7 are also given in Table 4. It is seen from this table that the result is rather insensitive to the assumed longitudinal gluon fragmentation function and to whether or not energy-momentum of the events is exactly conserved. Possible systematic errors were searched for by selecting different orientations of the sphericity axis and of the event plane within the drift chamber volume. Systematic errors were found to be smaller than statistical ones.

The results computed from the LUND string model, as shown in Fig. 7 and Table 4, are in rough agreement with the data and are insensitive to reasonable changes of the string fragmentation parameter σ_q.

6. Summary and Conclusions

We investigated fragmentation properties of 3-jet events selected from 18 846 hadronic e^+e^- annihilation events at $\bar{W}$ = 34.6 GeV. These 3-jet events, if interpreted as $e^+e^- \to q\bar{q}g$, offer the possibility to study the gluon jet. Two different concepts of fragmentation were considered: the independent jet (IJ) model and the LUND color string model. The parton dynamics was represented by 2nd order perturbative QCD. The

QCD + fragmentation models provide a good description of the angular distributions of the 3 jet axes.

A detailed study of the particle distribution in the event plane of 3-jet events was undertaken. The jets were ordered according to their energy such that $E_1 > E_2 > E_3$. From QCD one expects the third jet to be a gluon jet with about 55% probability. The production rate of soft ($p_{in} \lesssim 0.7$ GeV/c) particles in the angular gap between jets 1 and 2 relative to the rate in the other two gaps is found to be significantly lower than expected from independent parton fragmentation. The data is well reproduced by the LUND string model. In contrast to the soft particle region, at somewhat larger momenta ($0.7 \lesssim p_{in} \lesssim 1.7$ GeV/c) the IJ model describes the data better than the LUND model. We found that this discrepancy between the data and the LUND model is mainly associated with events of relatively low planarity ($Q_2 - Q_1$). Apart from this discrepancy, we confirm the earlier results of the JADE [5] and PEP-4 TPC [6] collaborations who presented clear evidence for string-like effects in 3-jet events.

In a second method we measured the systematic change of the three jet directions upon variation of a momentum dependent weight factor which was introduced into the calculation of the jet axes. This method is not restricted to the particles between jets and does not require identification of the gluon jet. Emphasizing soft particles, the data clearly prefer the LUND model over the IJ model. If, however, the weight is put onto the hard particles, the data are found to lie in between the predictions of the two models. The agreement between the data and the LUND model improves if events with more than 3 jets are removed.

We searched for possible differences between quark and gluon jets with regard to the average transverse momentum squared $\langle p_{T\,out}^2 \rangle$ and $\langle p_{T\,in}^2 \rangle$. Within the context of the IJ model, the data are compatible with quark and gluon jets having the same $\langle p_T^2 \rangle$. The data are also compatible with the hypothesis that gluon jets have larger $\langle p_T^2 \rangle$ than quark jets within the parameter range $0.35 \lesssim \sigma_{q,g} \lesssim 0.50$ GeV/c and $\sigma_{q,q} = 0.35$ GeV/c fixed. This result is compatible with the evidence presented by the JADE collaboration [9] that gluon jets are broader than quark jets.

Acknowledgements

We gratefully acknowledge the efforts of the PETRA machine group and the support of the DESY directorate. We are grateful to Dr. T. Sjöstrand for the many useful discussions. We thank the Department of Energy and the University of Wisconsin for providing the VAX 11-780 computer on which a large part of the extensive Monte Carlo calculations for this analysis were performed. Those of us from outside DESY wish to thank the DESY directorate for the hospitality extended to us while working at DESY.

List of References

1. TASSO Collaboration, R. Brandelik et al., Phys. Lett. 86B, 243 (1979);
MARK J Collaboration, D. P. Barber el al., Phys. Rev. Lett. 43, 830 (1979);
PLUTO Collaboration, C. Berger et al., Phys. Lett. 86B, 418 (1979);
JADE Collaboration, W. Bartel et al., Phys. Lett. 91B, 142 (1980).

2. MARK J Collaboration, D. P. Barber et al., Phys. Lett. 89B, 139 (1979);
JADE Collaboration, W. Bartel et al., Phys. Lett. 91B, 142 (1980);
TASSO Collaboration, R. Brandelik et al., Phys. Lett. 94B, 437 (1980);
PLUTO Collaboration, C. Berger et al., Phys. Lett. 97B, 459 (1980).

3. P. Hoyer, P. Osland, H.-G. Sander, T. Walsh, P. Zerwas, Nucl. Phys. B161, 349 (1979);
A. Ali, E. Pietarinen, G. Kramer, J. Willrodt, Phys. Lett. 93B, 155 (1980).

4. B. Andersson, G. Gustafson, G. Ingelman, T. Sjöstrand, Physics Reports 97, 33 (1983).

5. JADE Collaboration, W. Bartel et al., Phys. Lett. 101B, 129 (1981);
Phys. Lett. 134B, 275 (1984).

6. PEP-4 TPC Collaboration, H. Aihara et al., Phys. Rev. Lett. 54, 270 (1985);
Z. Phys. C-Particles and Fields 28, 31 (1985).

7. B. R. Webber, Nucl. Phys. B238, 492 (1984);
G. Marchesini, B. R. Webber, Nucl. Phys. B238, 1 (1984).

8. A. Petersen, Talk given at the "Symposium on Multiparticle Dynamics". Lund, June 1984; DESY Report 84-082.
JADE Collaboration, W. Bartel et al., DESY Report 85-036.

9. JADE Collaboration, W. Bartel et al., Phys. Lett. 123B, 460 (1983);
Z. Phys. C-Particles and Fields 21, 37 (1983).

10. UA1 Collaboration, G. Arnison et al., Phys. Lett. 132B, 223 (1983).

11. UA2 Collaboration, P. Bagnaia et al., Phys. Lett. 144B, 291 (1984).

12. TASSO Collaboration, R. Brandelik et al., Phys. Lett. 113B, 499 (1982).

13. J. Bjorken, S. Brodsky, Phys. Rev. D1, 1416 (1970).

14. S. L. Wu, G. Zobernig, Z. Phys. C-Particles and Fields 2, 107 (1979).

15. F. A. Berends, R. Kleiss, Nucl. Phys. B177, 237 (1981); ibid. B178, 141 (1981).

16. A. Ali et al., Nucl. Phys. B167, 454 (1980).

17. K. Fabricius et al., Z. Phys. C-Particles and Fields 11, 315 (1982).

18. T. Sjöstrand, Computer Phys. Comm. 27, 243 (1982).

19. TASSO Collaboration, M. Althoff et al., Z. Phys. C-Particles and Fields 26, 157 (1984).

20. C. Peterson et al., Phys. Rev. D27, 105 (1983).

21. TASSO Collaboration, R. Brandelik et al., Phys. Lett. 117B, 135 (1982).

22. T. Sjöstrand, DESY-Report 84-023.

23. B. Andersson, G. Gustafson, T. Sjöstrand, Phys. Lett. 94B, 211 (1980).

24. H. Daum, H. Meyer, J. Bürger, Z. Phys. C-Particles and Fields 8, 167 (1981).

IJ model	$\sigma_{q,q}$ (GeV/c)	$\sigma_{q,g}$ (GeV/c)	a_q	a_g	Remarks
1	0.35	0.20	0.61	0.61	$g \neq q$
2	0.35	0.35	0.61	0.61	$g = q$
3	0.35	0.50	0.61	0.61	$g \neq q$
4	0.35	0.60	0.61	0.61	$g \neq q$
5	0.35	0.35	0.61	2.0	$g \neq q$
6	0.35	0.35	0.61	0.61	$g \neq q$, $g \rightarrow q\bar{q}$
7	0.35	0.35	1.0	1.0	$g = q$
8	0.35	0.35	0.61	0.61	$g = q$ E, p conservation not imposed

Table 1 : Parameters for the independent jet model calculations

	N(2)/N(3)	N(1)/N(3)
Data	1.19 ± 0.03	1.51 ± 0.04
Lund model	1.28 ± 0.02	1.60 ± 0.03
IJ models:		
2 g=q	1.01 ± 0.02	1.17 ± 0.02
5 a_g=2	1.02 ± 0.02	1.16 ± 0.02
6 g→$q\bar{q}$	1.02 ± 0.02	1.21 ± 0.02
3 $\sigma_{q,g}$=.50	1.03 ± 0.02	1.15 ± 0.02
7 a_q=a_g=1.0	0.99 ± 0.02	1.09 ± 0.02
8 E, p conserv. not imposed	0.98 ± 0.01	1.08 ± 0.02
4- and 5-jet events excluded:		
Data	1.26 ± 0.04	1.64 ± 0.05
Lund model	1.31 ± 0.02	1.66 ± 0.03
IJ g=q model	1.02 ± 0.02	1.20 ± 0.02

Table 2 : Ratios of particle flow into the gap regions between jets for data and different fragmentation models. The errors are statistical only.

	$\langle \Delta x_T^{(1)} \rangle$	$\langle \Delta x_T^{(3)} \rangle$
Data	13 ± 8	29 ± 4
Lund model	24 ± 4	16 ± 2
IJ models:		
2 g=q	-63 ± 4	48 ± 2
5 a_g=2	-67 ± 4	50 ± 2
6 g→$q\bar{q}$	-62 ± 4	50 ± 2
3 $\sigma_{q,g}$=0.5	-56 ± 4	46 ± 2
7 a_q=a_g=1	-68 ± 5	50 ± 3
8 E, p conserv. not imposed	-77 ± 4	71 ± 3
4- and 5-jet events excluded:		
Data	23 ± 8	19 ± 4
Lund model	26 ± 4	12 ± 2
IJ g=q model	-61 ± 4	45 ± 2

Table 3 : Results of the jet direction analysis for data and various models. All values have to be multiplied by 10^{-4}. The errors are statistical only.

	r_{out}	r_{in}
Data	1.01 ± 0.03	0.76 ± 0.03
Lund model		
σ_q = 0.32	0.99 ± 0.01	0.82 ± 0.01
σ_q = 0.35	0.98 ± 0.01	0.82 ± 0.01
IJ models:		
1 $\sigma_{q,g}$ = .20	0.90 ± 0.01	0.61 ± 0.01
2 .35	1.01 ± 0.02	0.70 ± 0.01
3 .50	1.09 ± 0.02	0.76 ± 0.01
4 .60	1.16 ± 0.02	0.76 ± 0.01
5 a_g=2	1.03 ± 0.02	0.71 ± 0.01
6 $g \to q\bar{q}$	1.04 ± 0.02	0.71 ± 0.01
7 a_q=a_g=1.0	0.98 ± 0.02	0.70 ± 0.01
8 E, p conserv. not imposed	1.00 ± 0.02	0.69 ± 0.01

Table 4 : Values of r_{out} and r_{in} as defined in the text for data and different fragmentation models. The errors are statistical only.

Figure Captions

Fig. 1 Definition of variables in the event plane (x,y) spanned by the 3 jets.
a) Jet directions and particle momenta.
b) Fractional transverse momentum x_T of jet 3 with respect to jet 1.

Fig. 2 Distributions of jet energies and angles for the 3-jet event sample selected by cuts (i)-(iv). Superimposed on the data (●) are the IJ g=q (---) and the LUND model (——) calculations.
a) Scaled visible jet energies x_{vis}; 3 entries/event.
b) The minimum angle between the jets, min Φ_{ij}.
c) Scaled jet energies x_{rec} reconstructed from the angles between jets; 3 entries/event. The dotted line represents the gluon contribution as calculated from the model. A jet was called a gluon jet if the parton closest in angle to that jet was a gluon.

Fig. 3 Distributions of the reduced azimuthal angles ψ_2', ψ_1' and ψ_3' of charged particles in the angular regions 2, 1 and 3. The Monte Carlo calculations of the IJ g=q (---) and of the LUND models (——) are normalized to the same number of 3-jet events as in the data.
a) All particles, b) only $x_{in} < 0.04$ particles,
c) only $0.04 < x_{in} < 0.10$ particles.

Fig. 4 Ratios of particle densities in the angular gaps between the jet axes, defined by $0.25 < \psi_j' < 0.75$, as a function of x_{in}. The range $0 < x_{in} < 0.1$ is considered. The calculations of the IJ g=q and of the LUND models are shown as shaded bands. Only statistical errors are given.
a) N(2)/N(3) and b) N(1)/N(3) for the 3-jet event sample.
c) N(2)/N(3) requiring in addition $P = Q_2 - Q_1 < 0.07$, leaving 716 data events.
d) N(2)/N(3) requiring in addition $P = Q_2 - Q_1 > 0.07$, leaving 1645 data events.

e) N(2)/N(3), > 3 jet events excluded, leaving 2105 data events.

Fig. 5 The quantity $\langle \Delta x_T^{(n)} \rangle = \langle x_T^{(2)} - x_T^{(n)} \rangle$ for different values of n, where n=2 is chosen as reference point. The calculations of the IJ g=q and of the LUND models are shown as shaded bands.
a) for the 3-jet event sample,
b) as for a) but 4- and 5-jet events removed.

Fig. 6 Distribution of $\Delta x_T^{(1)} = x_T^{(2)} - x_T^{(1)}$ for the 3-jet event sample. Also shown are the IJ g=q (---) and the LUND (——) model calculations.

Fig. 7 The ratios r_{out} and r_{in} as defined in the text for the data (horizontal band) and for the IJ model (I) as a function of $\sigma_{q,g}$. Also shown is the result of the LUND model (L) for which the horizontal scale is irrelevant.

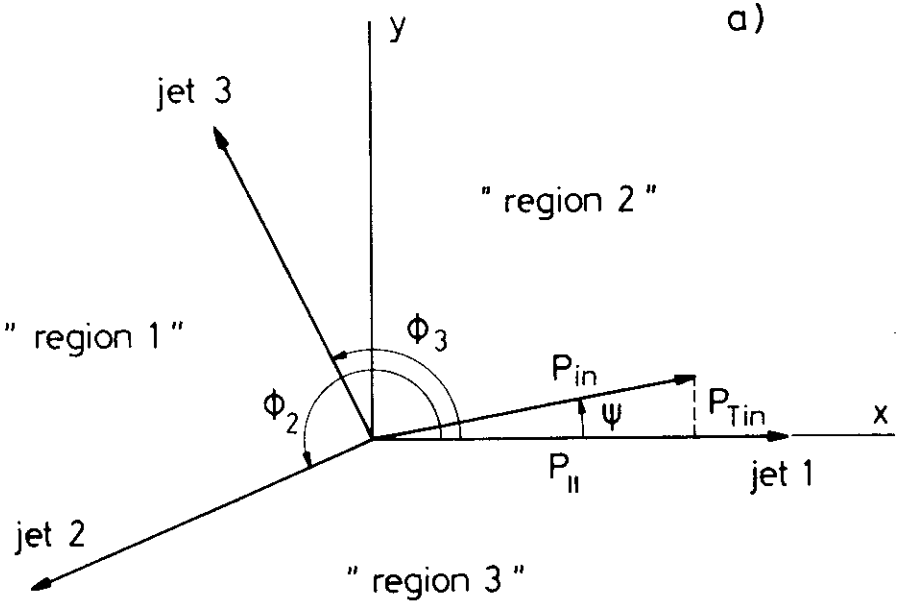

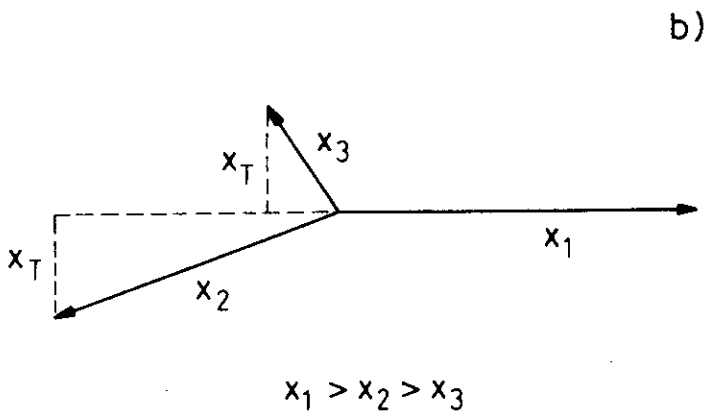

Fig. 1

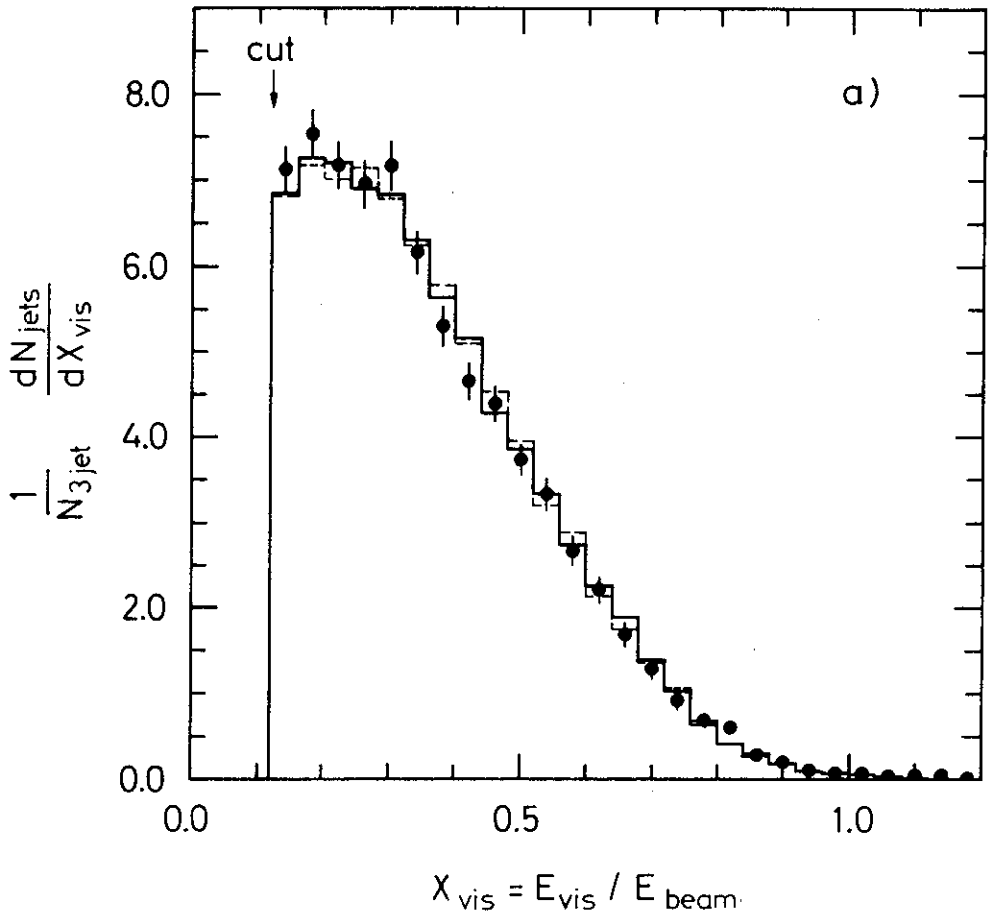
cut
a)
8.0
6.0
4.0
2.0
0.0
0.0
0.5
1.0
$\frac{1}{N_{3jet}} \frac{dN_{jets}}{dX_{vis}}$
$X_{vis} = E_{vis} / E_{beam}$

Fig. 2

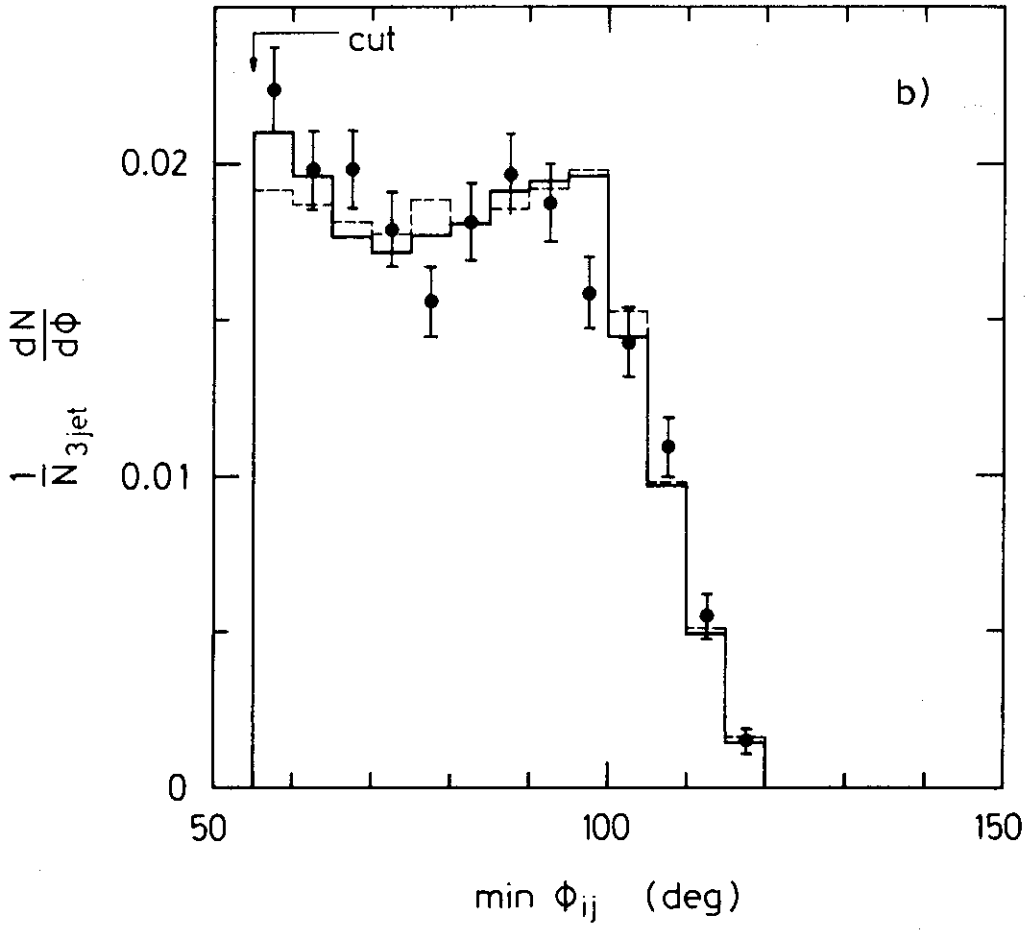
cut
b)
0.02
0.01
0
50
100
150
$\frac{1}{N_{3jet}} \frac{dN}{d\phi}$
min ϕ_{ij} (deg)

Fig. 2

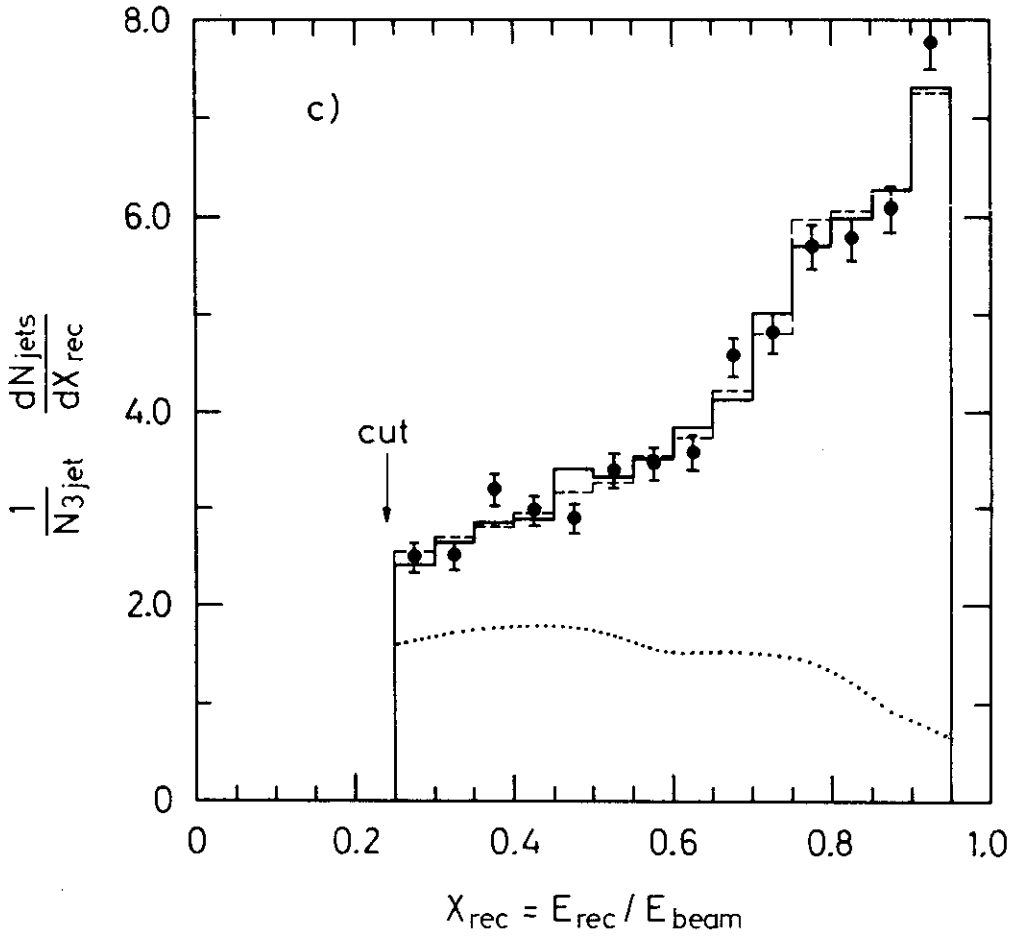
c)
cut
8.0
6.0
4.0
2.0
0
0
0.2
0.4
0.6
0.8
1.0
$\frac{1}{N_{3\,jet}} \frac{dN_{jets}}{dX_{rec}}$
$X_{rec} = E_{rec} / E_{beam}$

Fig. 2

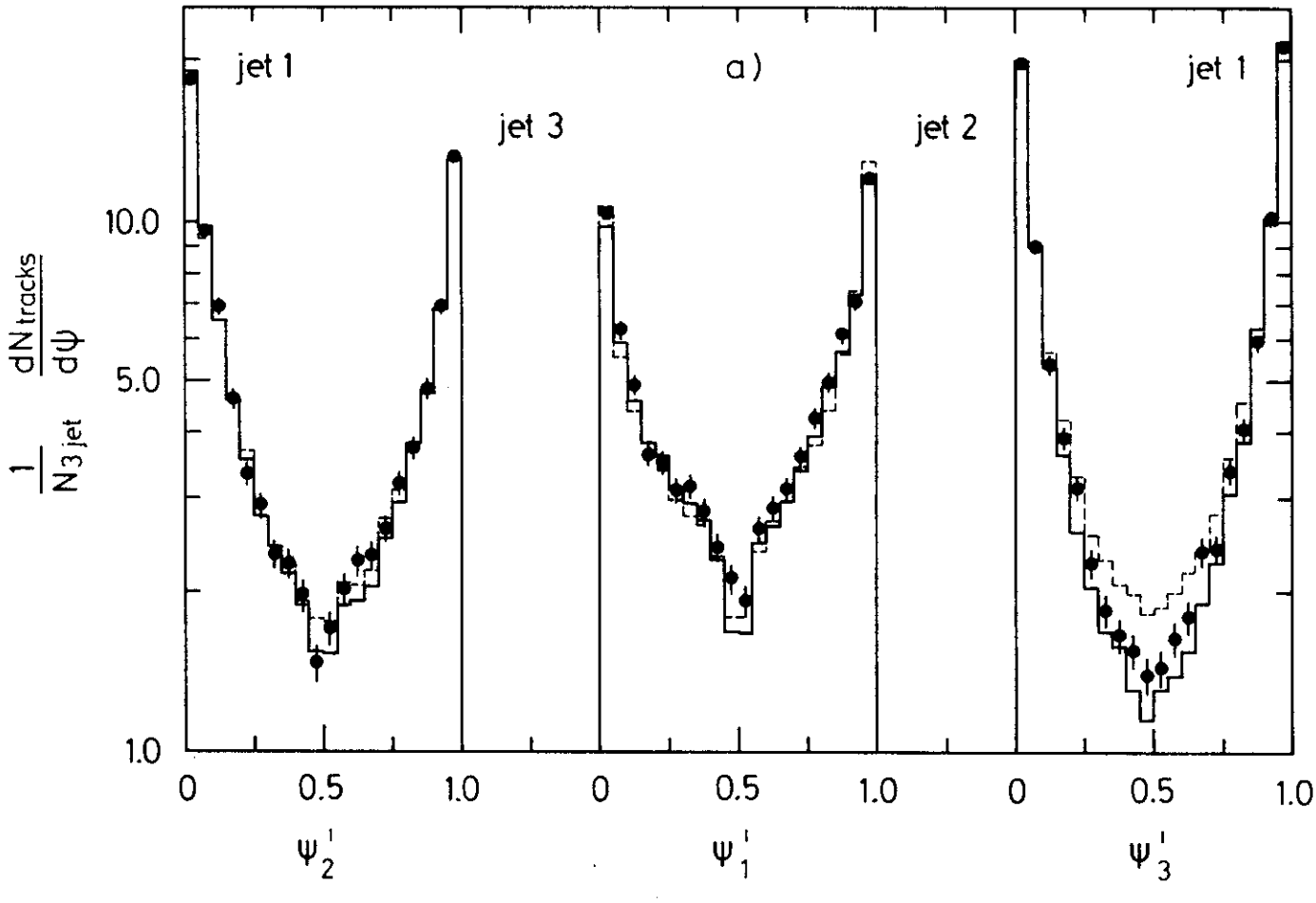
jet 1
jet 3
a)
jet 2
jet 1
10.0
5.0
1.0
0
0.5
1.0
$\frac{1}{N_{3\,jet}} \frac{dN_{tracks}}{d\psi}$
ψ'_2
ψ'_1
ψ'_3

Fig. 3

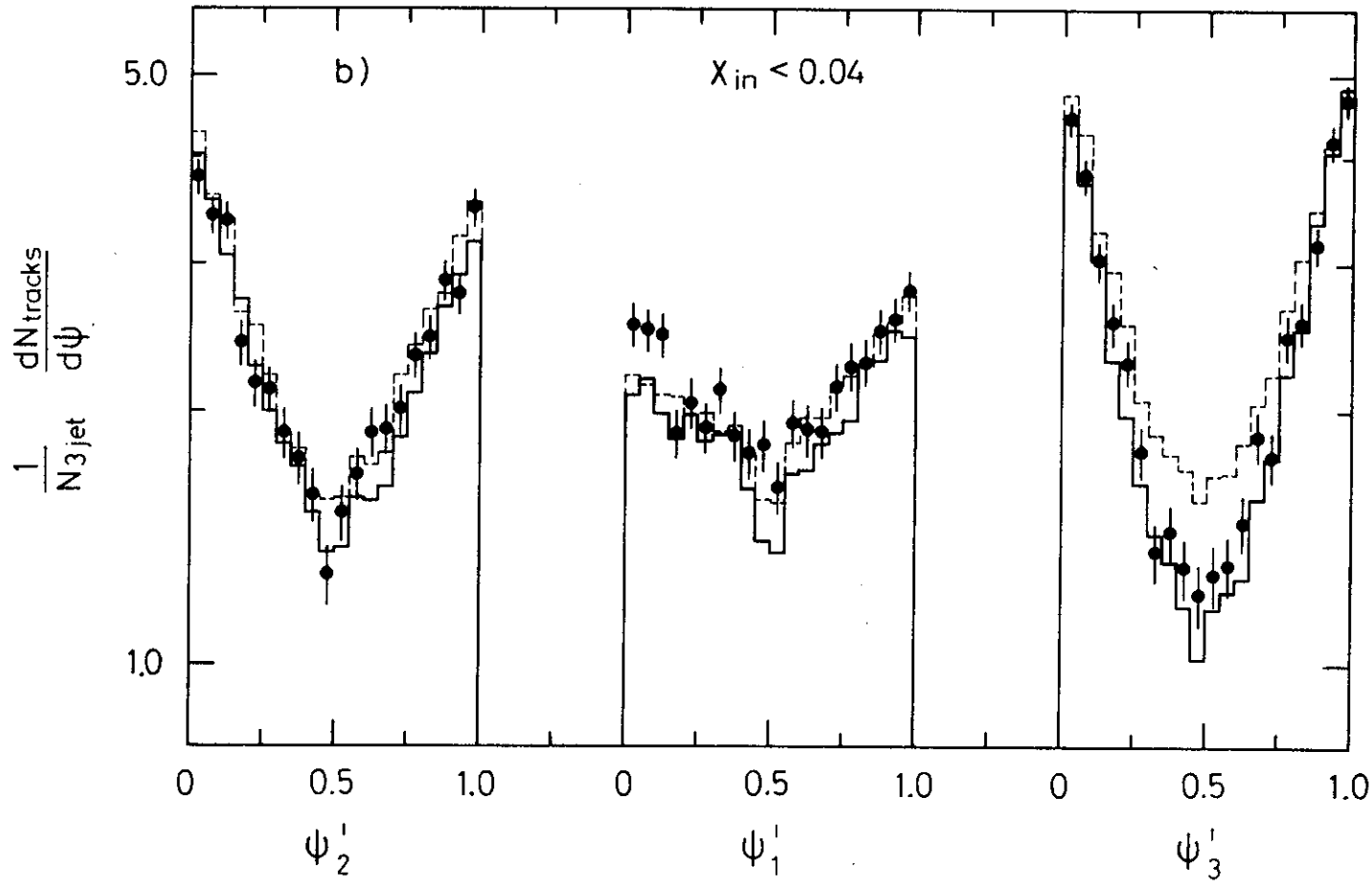
b)
$X_{in} < 0.04$
5.0
1.0
$\frac{1}{N_{3\,jet}} \frac{dN_{tracks}}{d\psi}$
0
0.5
1.0
ψ'_2
ψ'_1
ψ'_3

Fig. 3

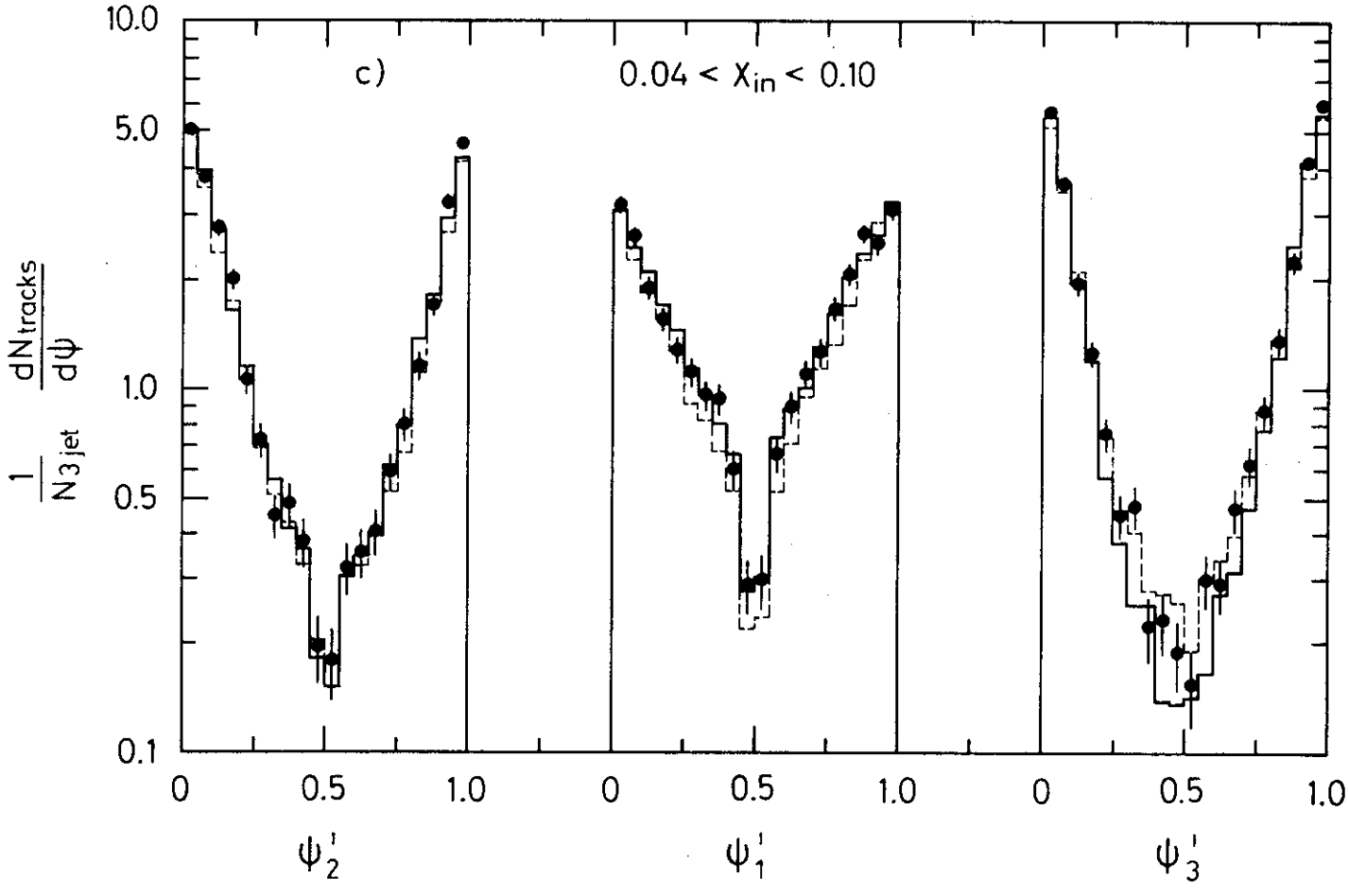
c)
$0.04 < X_{in} < 0.10$
10.0
5.0
1.0
0.5
0.1
$\frac{1}{N_{3\,jet}} \frac{dN_{tracks}}{d\psi}$
0
0.5
1.0
ψ'_2
ψ'_1
ψ'_3

Fig. 3

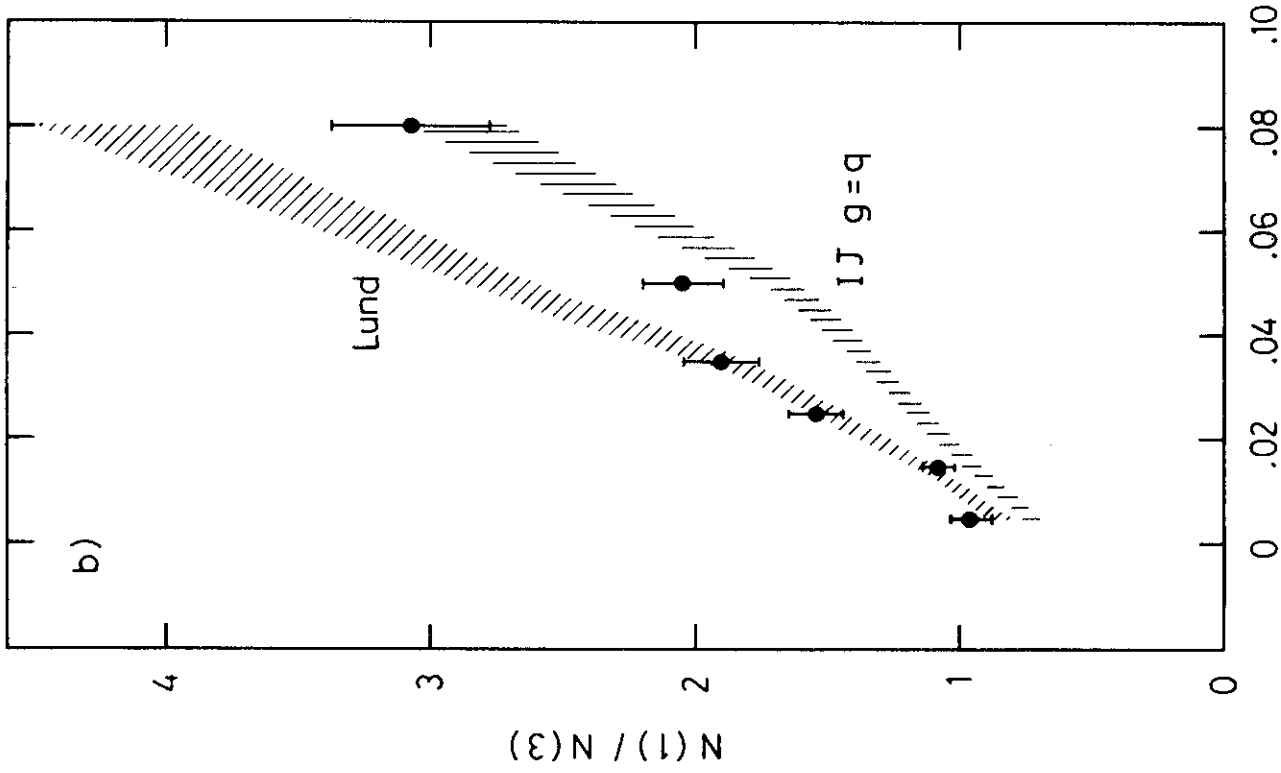

Fig. 4

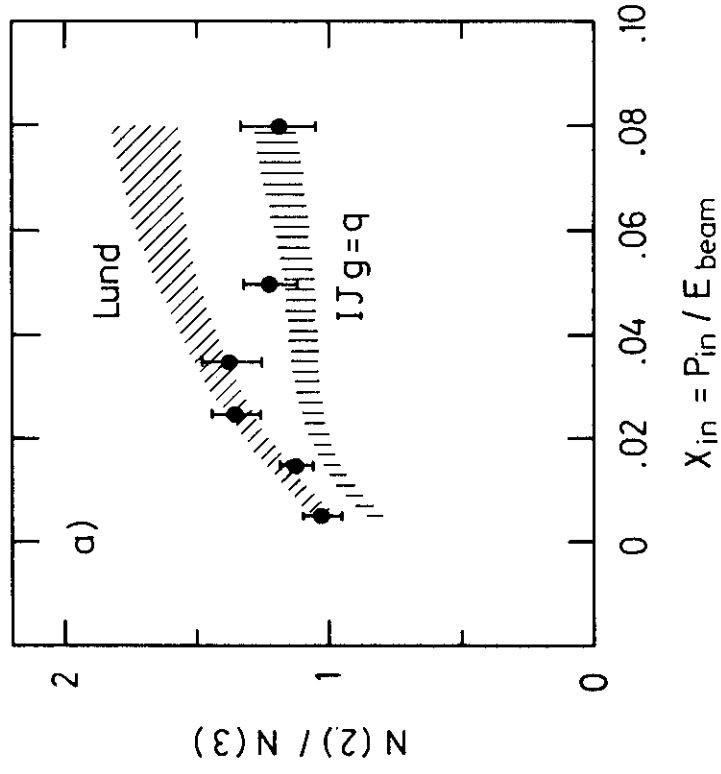

Fig. 4

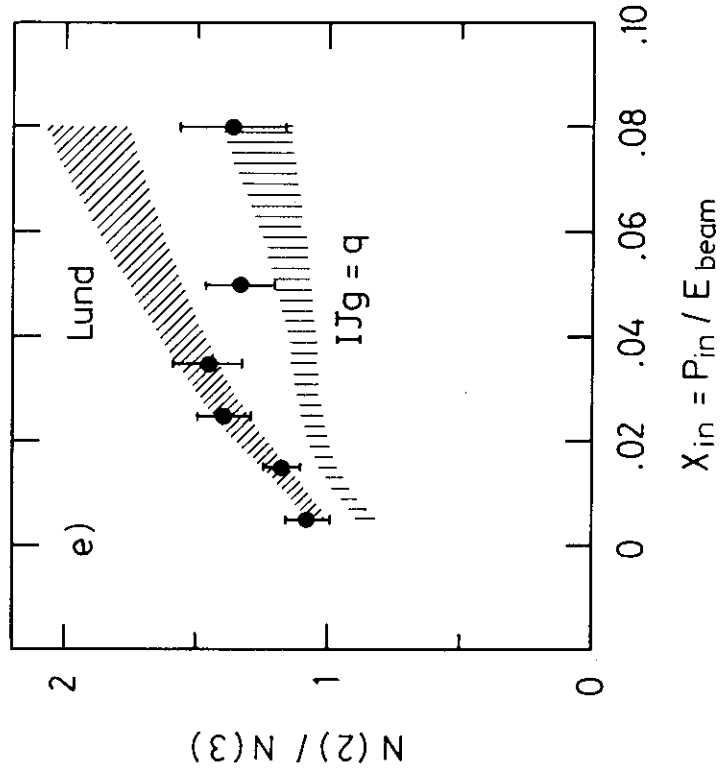
e)
Lund
IJg = q
N(2) / N(3)
$X_{in} = P_{in} / E_{beam}$

Fig. 4

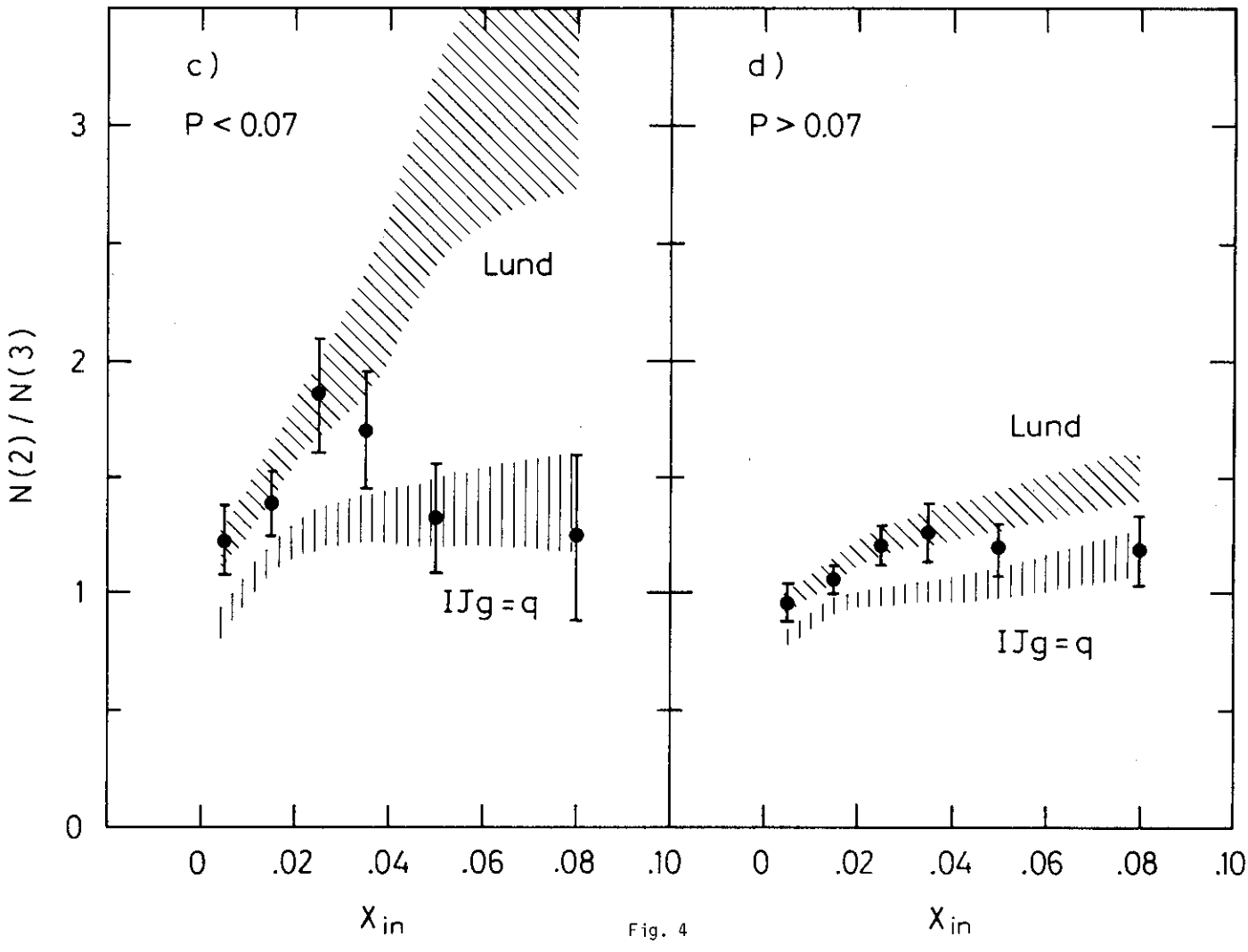
c)
P < 0.07
Lund
IJg = q
d)
P > 0.07
Lund
IJg = q
N(2) / N(3)
X_{in}
X_{in}

Fig. 4

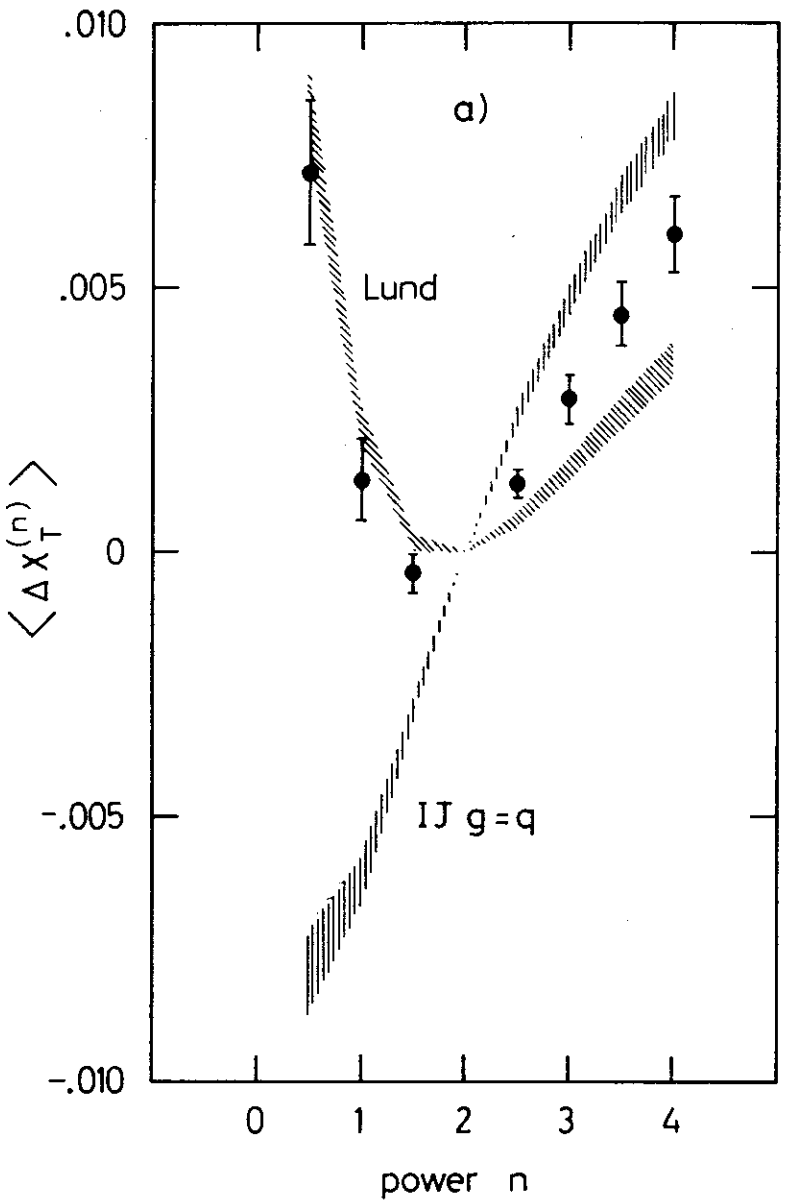
.010
.005
0
-.005
-.010
a)
Lund
IJ g=q
$\langle \Delta X_T^{(n)} \rangle$
0
1
2
3
4
power n

Fig. 5

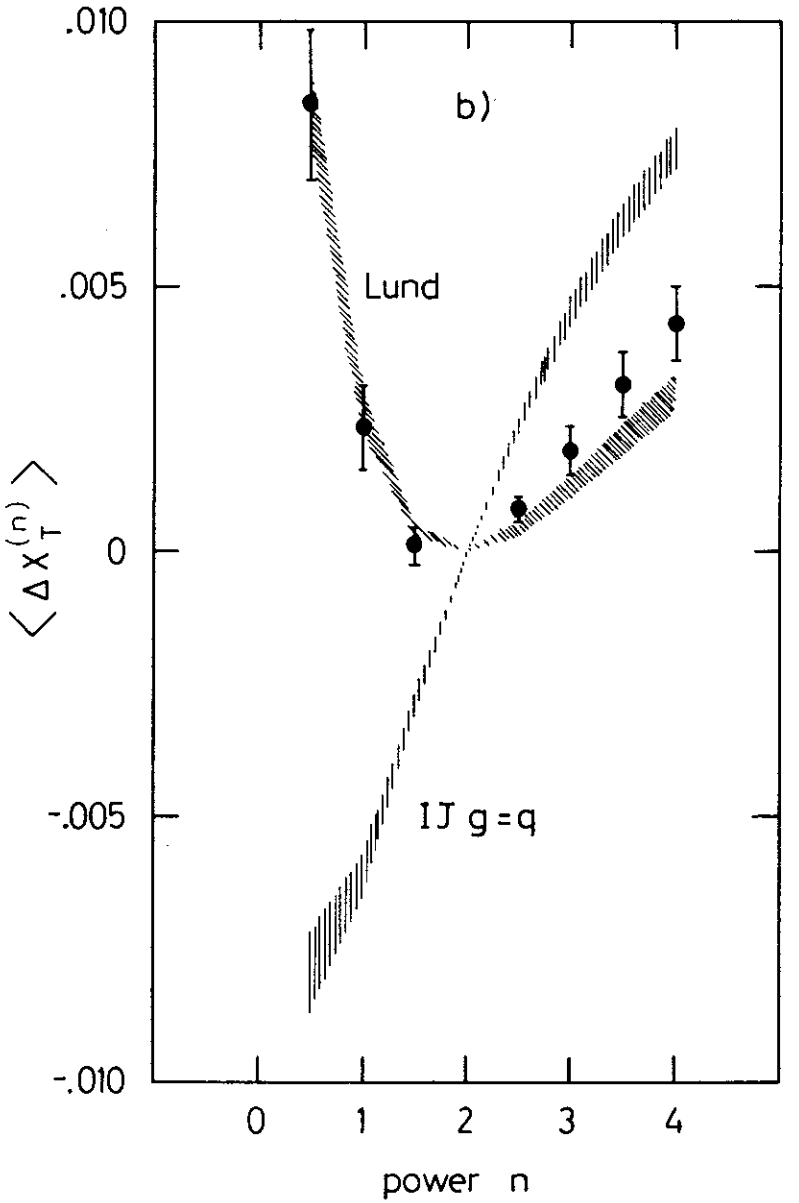
.010
.005
0
-.005
-.010
b)
Lund
IJ g=q
$\langle \Delta X_T^{(n)} \rangle$
0
1
2
3
4
power n

Fig. 5

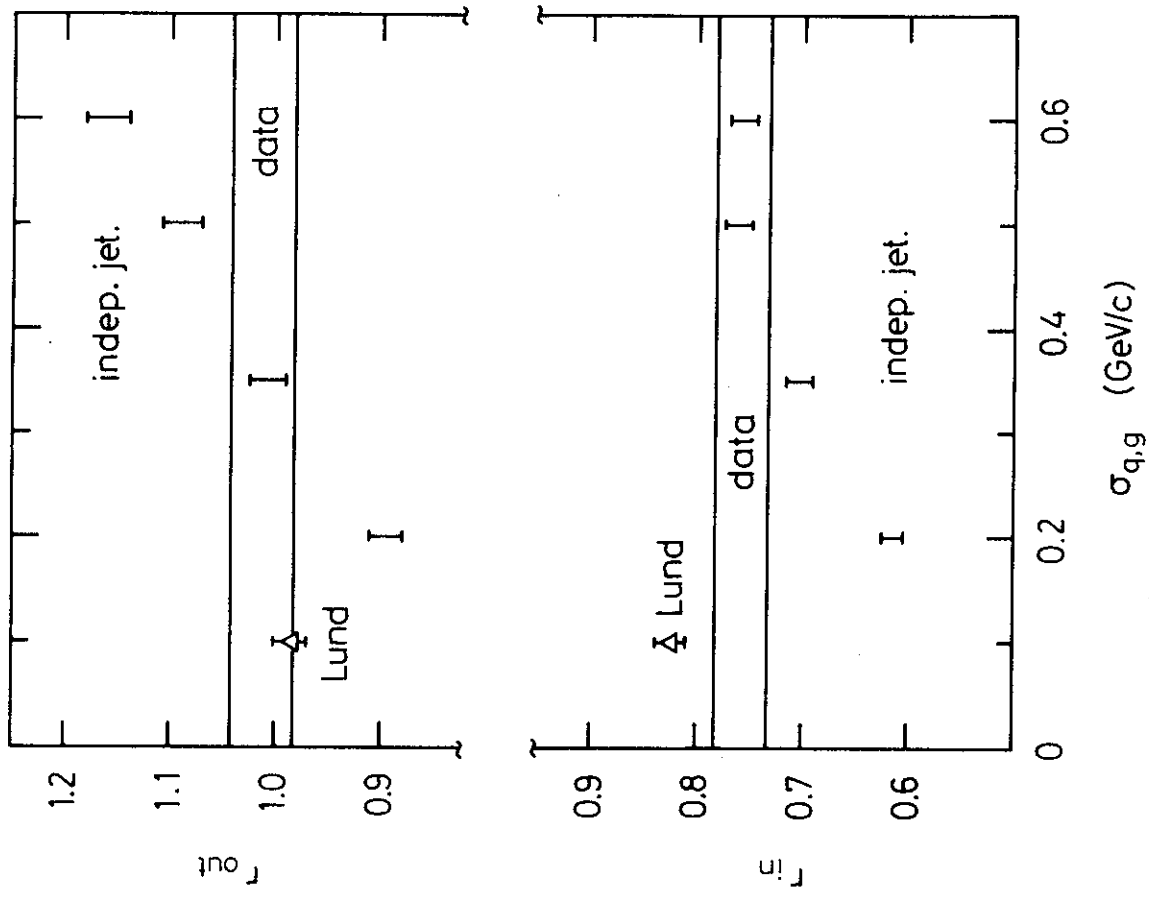
indep. jet.
data
Lund
1.2
1.1
1.0
0.9
r_{out}
Lund
data
indep. jet.
0.9
0.8
0.7
0.6
r_{in}
0
0.2
0.4
0.6
$\sigma_{q,g}$ (GeV/c)

Fig. 7

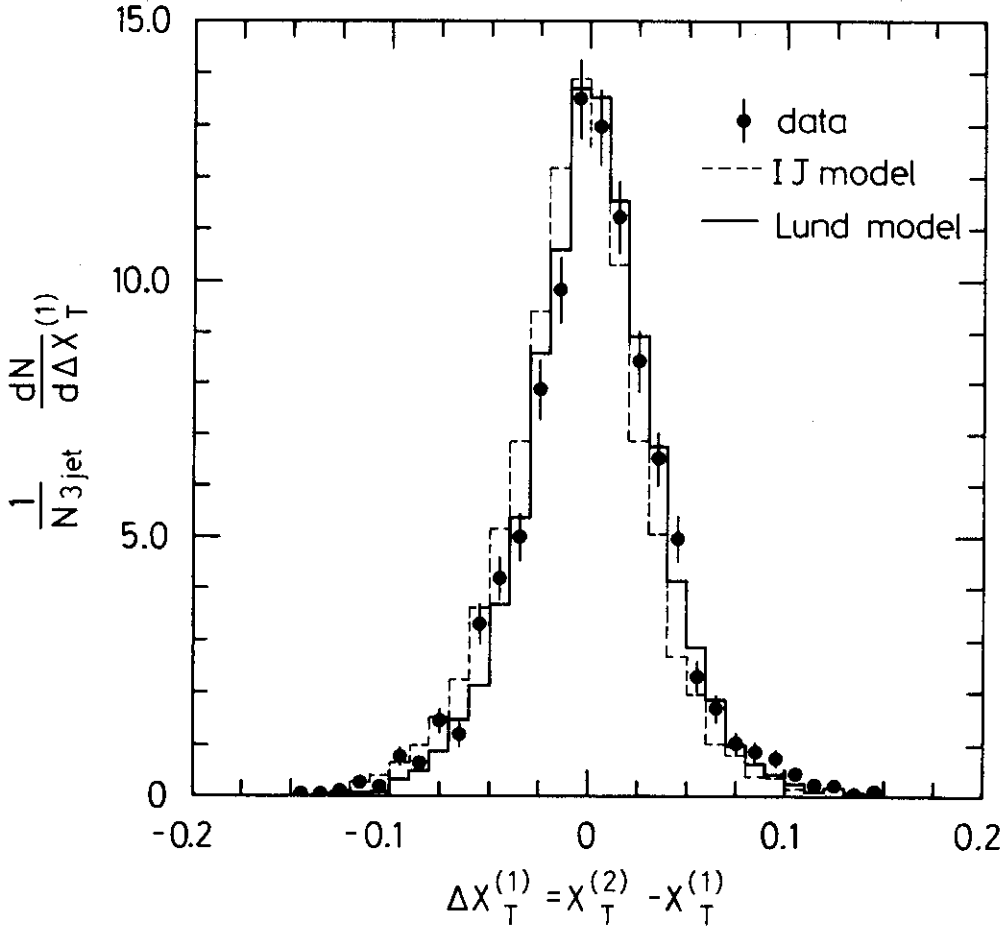
15.0
10.0
5.0
0
data
I J model
Lund model
$\frac{1}{N_{3jet}} \frac{dN}{d\Delta X_T^{(1)}}$
-0.2
-0.1
0
0.1
0.2
$\Delta X_T^{(1)} = X_T^{(2)} - X_T^{(1)}$

Fig. 6